LABORATORI NAZIONALI DI FRASCATI
SIS-Pubblicazioni

LNF-00/028 (P)
6 Novembre 2000

Measurements of Coherent Diffraction Radiation and its Application for Bunch Length Diagnostics in Particle Accelerators

M. Castellano[1], L. Catani[2], A. Cianchi[2], G. Orlandi[2], M. Geitz [3], V.A.Verzilov[1]
[1)] *INFN, Laboratori Nazionali di Frascati, P.O. Box 13, I-00044 Frascati, Italy*
[2)] *Istituto Nazionale di Fisica Nucleare, Roma 2,*
Via della Ricerca Scientifica 1, I-00133 Roma, Italy
[3)] *Deutsches Electronen Synchrotron, D-22603 Hamburg, Germany*

Abstract

Measurements of coherent diffraction radiation from a slit of a variable width generated by short electron bunches were performed in millimeter and submillimeter range. Experimental data are compared with transition radiation case and theoretical predictions. More realistic description, than the conventional theory does, is necessary to correctly account for the data. No noticeable difference in the bunch length value was observed between the diffraction radiation mode in a wide range of the slit widths and transition radiation one in the bunch length evaluation.

PACS.: 41.60.-m, 41.85.Ew, 41.75.Ht

Submitted to Physical Review E

1 INTRODUCTION

The development of the next generation of high luminosity electron - positron Linear Colliders and short-wavelength Free Electron Lasers requires electron pulses of ever higher peak current. This can be obtained by the use of a series of magnetic compressors working at intermediate energies to avoid emittance blow-up. An accurate measurement of sub-millimeter bunch lengths is thus necessary at every stage for a good setting of the compressor parameters.

Since standard time domain measurements become difficult and expensive to realize in this bunch length range, in recent years a frequency domain technique based on the measurement of the coherent radiation spectrum emitted by the beam under different conditions has been developed. Coherent synchrotron radiation (CSR) [1,2] and coherent transition radiation (CTR) [3,4] are the most used radiation sources.

Coherent emission occurs at wavelengths comparable with, or longer than, the bunch length when all electrons in the bunch produce radiation more or less in phase. The coherent spectrum of a bunch of N electrons is given by the product of the single particle spectrum $S(\omega)$ and the bunch form-factor $F(\omega)$ containing information about the bunch spatial dimensions

$$S_{coh}(\omega) = N^2\, S(\omega)\, F(\omega)\,. \tag{1}$$

If CSR is generally used at circular accelerators, CTR has become one of the basic diagnosing tool at linacs and transfer lines in the last decade. Despite of certain limitations, the latter is now well mastered, and its accuracy improves as shorter bunches become available. A serious problem will arise with high-power density beams capable of damaging screens, used to produce radiation, by ionization heating. Because this problem is inherent to all intercepting diagnostics, like SEM grids or wire-scanners, the next generation of low-emittance and high-power beams needs new non-intercepting diagnostic devices to be developed.

As a possible solution, the use of coherent diffraction radiation (CDR) for bunch length measurements was suggested [5,6]. Diffraction radiation arises when a charged beam passes through an aperture in a metallic screen, effects of the beam interaction with the screen material can, therefore, be minimal and a smaller perturbation to the beam is produced compared with most of other diagnostics.

So far there was only a single experimental evidence of CDR [7]. However, due to the experimental lay-out, the detected radiation was a superposition between forward diffraction radiation from a circular hole and transition radiation produced by the beam on a mirror used to extract the former from a vacuum chamber. The result shows interference of the two radiations . The characteristics of CDR could only be obtained by subtracting

theoretically evaluated CTR ones. In these evaluations, as was pointed out in [8], the crucial (under conditions of the experiment) effect of the screen finite size was not taken into account.

In this paper we present the first "clean" bunch length measurement using CDR generated by short bunches crossing a variable width horizontal slit, and compare it with that based on CTR, taken with the same apparatus and under the same experimental conditions. Some DR properties, such as the intensity dependence on the slit width, are tested against theoretical predictions. We will show that a realistic theoretical description is required to correctly account for the measured data.

2 THEORETICAL BACKGROUND

In the most general sense diffraction radiation (DR) is a radiation produced by uniformly moving sources of electrical and magnetic fields in proximity of optical discontinuities, i.e. of objects that can reflect, refract or scatter electromagnetic waves. The list of phenomena covered by such a "global" definition, however, is truly inexhaustible. Fortunately, the cases that have significant practical interest for beam diagnostics are well known and almost uniquely limited to that of DR emerging when charged particles pass near the edges of or through simply shaped apertures in thin conducting screens. This class of DR problems has been intensively studied theoretically since the end of the fifties (see, e.g. reviews [9–11] and references therein).

The theory of DR has much in common with the well known theory of diffraction of free electromagnetic waves. Normally, this fact finds its explanation in the picture representing the field of a charged particle moving at a constant velocity as a superposition of plane waves of various frequencies (pseudophotons). All these waves propagate at the same speed as the particle and are exponentially damped with increasing distance from the particle trajectory. One can say that they are locked to the charge and can not travel independently. As the particle in motion meets optical discontinuities, some of the pseudo waves can be scattered by obstacles giving rise to undamped waves, i.e. to radiation.

DR has, however, some peculiar features. In contrast to an ordinary plane wave, the field of a charged particle depends on the distance from it. If one considers a Fourier component of this field of wavelength λ at a distance r from the particle trajectory, one can see that it becomes negligibly small when $r \geq \lambda\gamma$, where γ is the particle Lorentz factor. In other words one can say that pseudophotons of a wavelength λ are confined within a disk of a radius $r \sim \lambda\gamma$. It is, therefore, natural that the interaction of the charge field of the given wavelength with an obstacle is characterized by the ratio of the obstacle dimensions (or the distance from the screen edge to the particle trajectory) to

the parameter $\lambda\gamma$. In the case of the particle passing through the centre of an aperture of size a in an opaque screen, DR is strongly suppressed at wavelengths $\lambda \leq a/\gamma$. At such wavelengths all goes as if the screen was not there.

Application of exact methods to DR problems is normally associated with enormous difficulties in calculations (see, e.g. [9]). Approximations are widely used instead, and even so analytical solutions are not always found. Simple far-field expressions are derived in Ref. [11] on the basis of the well-known Huygens principle for DR from circular apertures and slits in infinite, perfectly conducting, thin screens. However, under real conditions, both far-field and infinite screen approximations may not be applicable for long wavelengths and sufficiently large γ. The role of the screen size in regard to transition radiation (TR) was shown for the first time in Ref. [8] and later in Refs. [12,13]. It was found that TR spectra change when the parameter $\lambda\gamma$ exceeds the transverse dimensions of the emitting screen. If the screen is round with outer radius r, strong suppression of the radiation occurs at wavelengths $\lambda \geq r/\gamma$. It is evident that these arguments are valid also in the case of DR, where both low-frequency and high-frequency intensity reductions may be observed at the same time. Screen finite size effects along with diffraction in the collecting optics and corrections to the far-field approximation were considered in Ref. [13] in the context of bunch length measurements based on coherent TR emission. The results of this work can be easily extended to the case of DR and the geometry of the present experiment.

3 EXPERIMENTAL SET-UP

The experiment was performed at the TESLA Test Facility superconducting linac at DESY. In the current configuration the linac comprises the laser driven rf gun, the capture cavity and two accelerating modules followed by a 15 m long undulator section. Bunch compressor II, a magnetic chicane located in between the two modules, is used to shorten the bunches longitudinally to sub-millimetre lengths. The experimental station for bunch length measurements is placed in between the second accelerating module and the undulator. The radiation produced by 225 MeV electrons on the surface of a diffraction screen (radiator) oriented at 45° to the beam axis is extracted from the vacuum pipe at 90° through a quartz window and analysed by means of a Martin - Puplett interferometer. During measurements the linac was operated in the single-bunch mode to avoid saturation of the detector. The bunch charge was 1 nC.

3.1 Diffraction radiator

Several constrains have led to the present design of the diffraction radiator. The device has to fit the space that formerly housed a standard TR screen, to avoid major modifications of the vacuum chamber of the TTF linac. It must function as a normal TR screen for transverse beam profile analysis as well. For these, and other practical reasons, we made the radiator in the form of a variable width slit, i.e. a rectangular metallic screen divided in two coplanar halves movable one with respect to the other. The whole device can be inserted in or removed from the beam line like a standard screen. So that, when the two parts are closed together it operates as an TR radiator. In the DR mode, the slit aperture can be adjusted depending on the beam size and positioned with respect to the beam by means of two independent coaxial UHV linear actuators driven by stepping motors. A resolution of 5 μm/step was achieved for the insertion motion and of 2.5 μm/step for the slit width variation in the range 0-10 mm.

For the two halves of the screen closed together to constitute an ideal radiator for transition radiation, they must present perfectly flat surfaces with parallel and straight edges. Tolerances for these parameters cannot be easily defined, depending strongly on the kind of measurements to be performed. In the actual case of bunch length measurements, in which a detailed analysis of the radiation angular distribution is not required, the flatness should be such that the error in the reflection angle is much smaller than the accepted solid angle, while the straightness and parallelism of the edges should be much less than the wavelength used.

Because from the expected parameters of the TTF beam, it follows that no wavelengths shorter than 0.5 mm are present in the coherent spectrum, we require the border straightness to be better than 100 μm, and because the angular acceptance of the interferometer is about 200 mrad, an overall planarity better than 20 mrad is sufficient.

Our standard OTR screen is a thin (8 μm) aluminized kapton foil stretched on a stainless steel frame. First attempts have shown that a straightforward application of the same technique to the diffraction radiator, having a three-sided rectangular frame, did not meet the above requirements: a stretched kapton foil always showed an unacceptably large curvature along its frame-free border, that could not be corrected even by increasing the foil thickness to 100 μm.

The problem was solved using a monocrystalline silicon wafers whose surface can be made very smooth and aluminized for higher reflectivity. The mechanical properties are also well compatible with our specifications.

For the present experiment a commercially available wafer of 380 μm thickness was used from which the two halves of the radiator were cut by means of a micrometric saw,

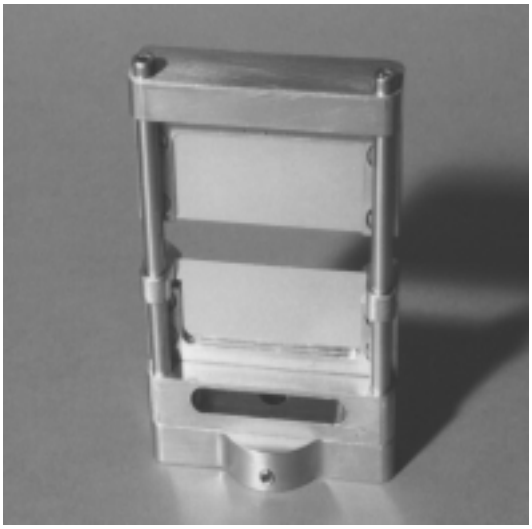

Figure 1: Diffraction radiator in the open position.

in the form of a 44 mm x 20 mm rectangle. The cut straightness was measured to be of the order of 20 μm, far below tolerance requirements. A picture of the two halves mounted on the frame in the open position is shown in Fig. 1.

The screen planarity was measured by scanning across the surface horizontally and vertically with a laser beam and observing the change in the spot position of the reflected beam at 2 m distance. The resolution of the measurement was 0.15 mrad. A concave curvature in the horizontal plane of ± 0.45 mrad was observed on both halves. Problems were also encountered to assure coplanarity between the two halves but for the present experiment the measured coplanarity angle of $\pm$ 3 mrad is acceptable.

In conclusion, owing to their mechanical and optical properties silicon wafers are a very promising material for diffraction radiators. However, in spite of the relatively low atomic number, the present screen thickness would still be excessive, because of the power deposited, for an intense beam such as that of TESLA. We have therefore started a research program for the production of much thinner diffraction screens, based on silicon wafers.

3.2 Interferometer

As sketched in Fig. 3.2 the DR screen is placed in the focus of a 200 mm focal length metallic parabolic mirror, that converts the diverging radiation fan, emerging from the quartz window, into a nearly parallel beam. A movable optical mirror allows to directly observe, with a vertically mounted camera, an image of the beam spot on the screen, for alignment purposes.

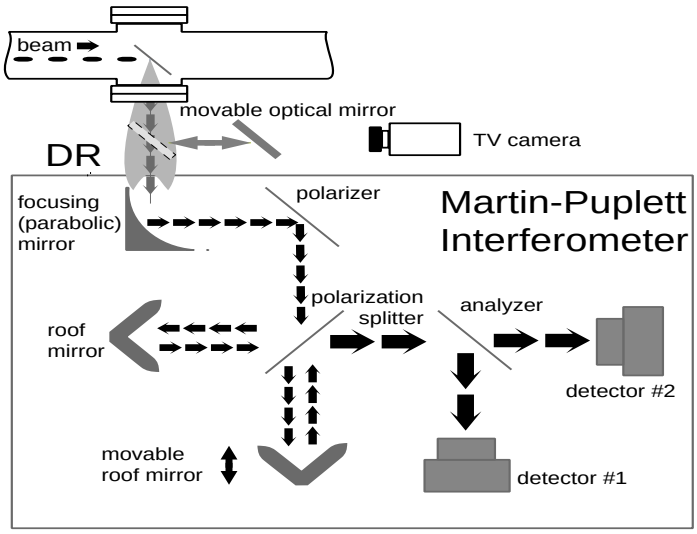

Figure 2: In the Martin - Puplett interferometer the orthogonal polarization components from a polarizating beam splitter go along the two different arms, are rotated by the roof mirrors and and recombine before reaching the detectors.

The wire grid polarizer , admitting transmission of the vertical polarization component of radiation, is the first element of a Martin-Puplett interferometer, developed and constructed by the University of Aachen and discussed in [15]. The Martin-Puplett is a two arms interferometer, similar to a Michelson one, in which the beam splitter is replaced by a 45° tilted polarizing grid splitter, so that orthogonal polarization components going along the two different arms are rotated by the roof mirrors and recombined before reaching the detectors. The possibility to measure both opposite sign polarization components allows a reduction of the measurement noise due to beam current fluctuations.

4 EXPERIMENTAL RESULTS AND DISCUSSION

4.1 Diffraction radiation properties

The known relation between CDR spectrum and that of incoherent DR allowed us to study some characteristics of the latter and test different theoretical models against measured data in regard to the horizontal slit width dependency.

Raw data in our measurements were interferograms registered by the two detectors for several slit widths in the range of 0 to 10 mm. The slit as a whole was always kept centered with respect to the beam ellipse measuring .5 mm (rms) vertically by 5 mm (rms) horizontally. The full set of interferograms for detector I is present in Fig. 3.

An interferogram shows the detector signal as a function of the optical path dif-

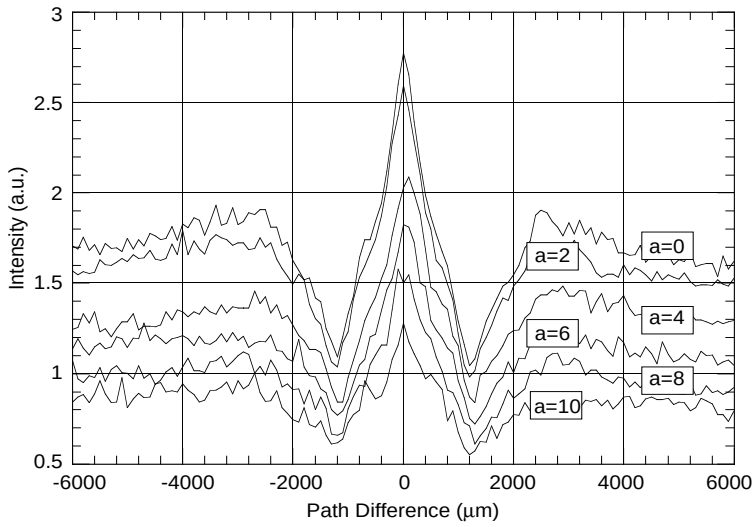

Figure 3: The detector I signal as a function of the optical path difference for various slit widths a.

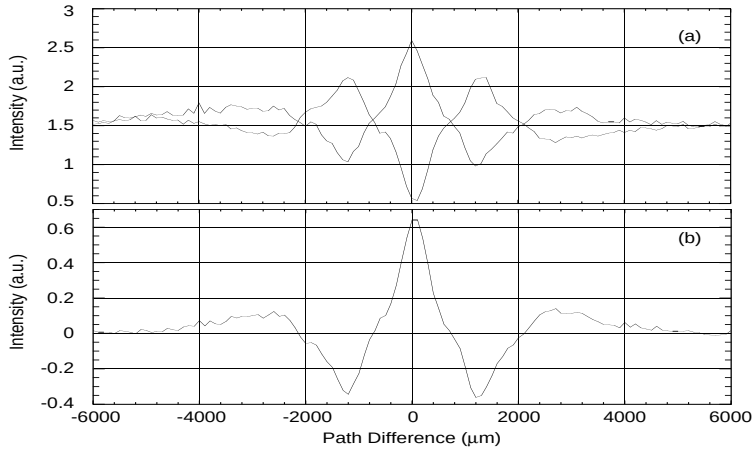

Figure 4: a) Interferograms measured at detectors I and II for the slit width $a = 2$ mm. b) The normalized autocorrelation curve obtained from the difference of the two detectors signals divided by their sum.

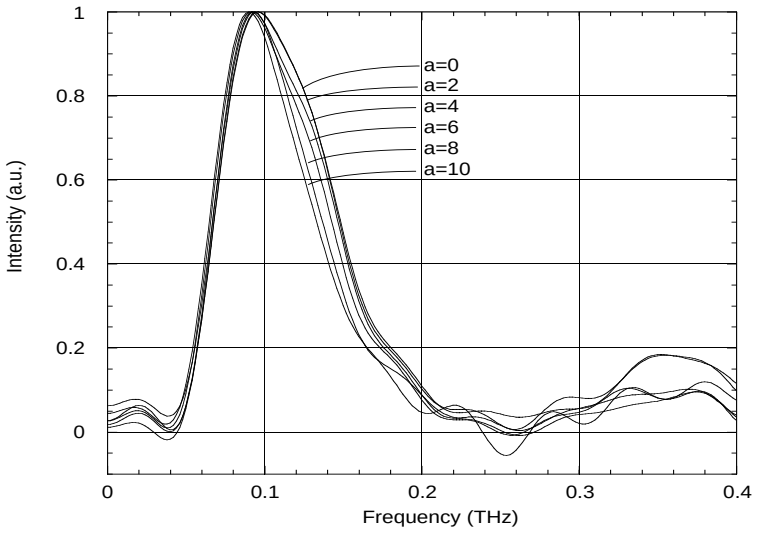

Figure 5: Normalized coherent radiation spectra for different slit widths a.

ference in the two interferometer arms. Hence, it consists of a variable autocorrelation component superimposed on a constant base-line proportional to the integrated power of the radiation pulse. Fig. 3 shows that the radiation intensity gradually decreases when the slit aperture increases, a behaviour expected from theory because the field is stronger near the particle, but the effect is wavelength dependent, as briefly discussed in the section 2, so that the shape of the DR spectrum should vary with the slit width.

Experimental spectra of CDR are obtained from the autocorrelation curves by Fourier transform. Thanks to the possibility of measuring both polarization components, the common noise, mainly due to beam current fluctuations, can be eliminated by taking the difference between the two signals and dividing it by the sum, so as to obtain a clean normalized autocorrelation curve. One of these curves for a=2 mm is shown in Fig. 4 as an example.

Beam CDR spectra derived from the autocorrelation curves are given in Fig. 5. Negative values in the spectra are due to the statistical noise and should be discarded. Statistical fluctuations, especially at higher frequencies, increase with the slit aperture as a consequence of the reduced signal intensity as the slit width becomes larger. All the spectra have an evident multiple peak structure. The shape of the coherent spectra reveals that the low-frequency part $\nu < 0.1$ THz is strongly suppressed. The behaviour in this frequency range is almost independent of the slit dimensions and, therefore, controlled by other experimental factors (detector spectral response, diffraction phenomena etc.). At higher frequencies weak deviations in the spectra for various slit widths can be attributed to radiation properties.

When considering theoretical predictions for incoherent DR spectra, we suspected that the widely cited results of Ref. [11] would not give a good description of measurements. There are several arguments, in part already mentioned above, to explain this. Firstly, the infinite screen approximation used in [11] is not fulfilled in our case. In fact, at wavelength 2-3 mm, where the maximum intensity of the CDR was detected, the parameter $\lambda\gamma$ is in a range of 900-1350 mm, that is much larger then the screen size. Hence, the effect of finite screen dimensions has to be taken into account. Secondly, formulae of Ref. [11] are valid for the far-field region. This implies that the radiation at the observation point is represented by an outgoing spherical wave and is equivalent to considering the source of the radiation to be point-like. The diverging beam from such a source would be transformed by the first parabolic mirror into a parallel one entering the interferometer itself. However, for the far-field approximation to be fully correct, the radiator and the interferometer should be separated by a distance much larger than $\lambda\gamma^2$. This is not the case for our experimental set-up. Generally, the source effective size is $\lambda\gamma$ or that of the screen, depending which is smaller, and the beam entering the interferometer is no longer parallel. Therefore, the real geometry of the measurement apparatus must be included in calculations in greater detail.

Both effects were considered in our previous work [13] using an approach equivalent to the Fresnel approximation in the diffraction theory of light. In the highly relativistic regime $\gamma \gg 1$, the power spectrum of the y - polarized radiation from the emitting screen placed in the front focal plane of a simple infinite lens with a focal length f and detected at a distance b behind the lens is given by

$$S_\omega = \frac{c}{4\pi^2}\int_{S_D} dxdy|E_y(x,y,\omega)|^2 \ , \tag{2}$$

$$\begin{aligned} E_y(x,y,\omega) &= \frac{iq}{\pi c}\frac{k}{f}\int_{S_s} dx_s dy_s \left[\alpha K_1(\alpha\rho_s) - \frac{J_0(k\rho_s)}{\rho_s}\right] \\ &\times \frac{y_s}{\rho_s}\, e^{i(k/2f)\rho_s^2(1-b/f)}\, e^{-i(k/f)(x_s x + y_s y)} \ , \end{aligned} \tag{3}$$

$$\rho_s = \sqrt{x_s^2 + y_s^2} \ , \ \alpha = k/\gamma \ . \tag{4}$$

where k is the wave vector, q the electron charge, c the velocity of light, $J_0(x)$ and $K_1(x)$ the Bessel and modified Bessel functions, respectively. The integration in Eq. (2) is performed over the detector aperture, while that in Eq. (4) is carried out over the screen surface.

Figure 6 shows the theoretical spectra calculated using Eqs. (2) and (4). In addition to the plain reduction in the intensity, there is a clear change in shape. Spectra for larger

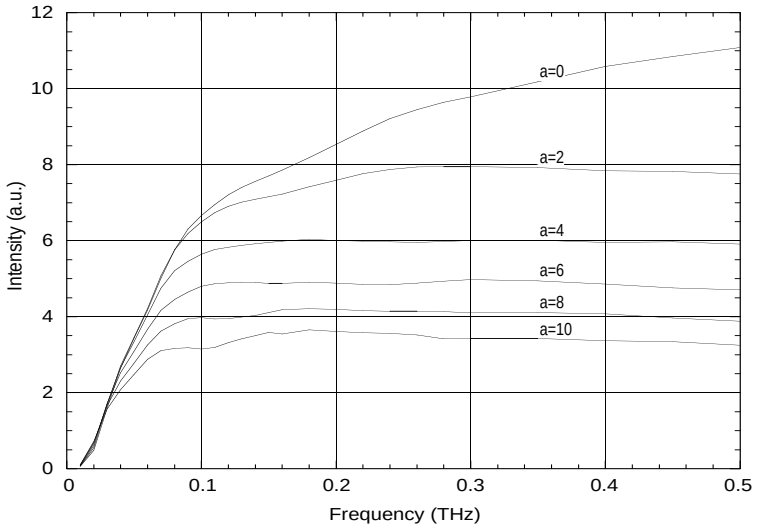

Figure 6: Incoherent diffraction radiation spectra for different slit widths a in the model taking into account screen size and corrections to the far-field approximation.

slit apertures become flatter as a consequence of the high frequency suppression due to the slit aperture and the low frequency cut-off moving slightly towards smaller frequencies as the outer screen dimensions grow (as a result of the increased slit width). The effect of the low-frequency radiation cut-off in the range of interest have been shown [14,13]to be a limiting factor leading to uncertainty in the bunch measurements. To this point, one can conclude that DR has even additional advantages (because of the spectrum shape) compared to TR from a screen of the same size, if the intensity is not a matter of concern.

The coherent power spectrum is related to the single particle one by a factor, insensitive to the slit width, that is the product of the beam form-factor and a frequency-dependent filter function characterising the spectral properties of the radiation transport channel and the detector spectral efficiency. The form - factor is a quantity to be determined while the filter function is very difficult to calculate, but their product can be derived from the measured spectra. For that we calculated the ratios of the measured coherent spectra to the corresponding theoretical single particle ones. They are shown in Fig. 7, normalized each to its maximum. As expected, curves for slit aperture from 0 to 6 mm are almost completely superimposed. The reason why it is not the same for slit widths of 8 and 10 mm is not yet understood but it could be due to the larger statistic noise contribution because of the lower intensity for large slit apertures and to a non perfect alignment causing a different angular acceptance for larger sources.

Since the $\lambda\gamma$ value was larger than the vacuum pipe radius, a possible source of background in the measurement could derive from wakefields emitted along the beam

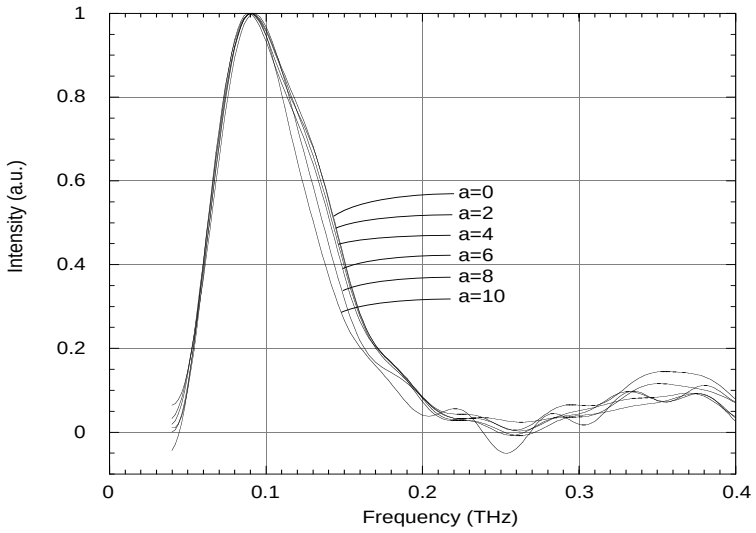

Figure 7: Experimental coherent spectra divided by theoretical incoherent ones should give rise to a " universal" curve independent of the slit width.

path and reflected by the screen. To verify this we compared the measured behaviour of the total coherent power as function of the slit aperture with theoretical expectations. Measured values of this quantity are simply given by the sum of the signals of the two pyroelectric detectors. In view of the absence of the absolute detector calibration, in Fig. 8 they are shown normalized to the case of the zero slit width (TR mode). Theoretical values were obtained by multiplying each of the appropriately normalized curves in Fig. 5 to the corresponding theoretical single particle spectra (Fig 6) followed by the integration over the frequency.

Experimental points and theoretical dependence for the radiation power are in a very good agreement. This can be regarded as an evidence of small contribution from the background mechanisms. On the other hand it is also an evident confirmation of our conjecture concerning the necessity of modifying the standard theory by including realistic elements (such as a screen size) in it. In fact, we did similar calculations using the classical formulae of Ref.[11]. The result is also shown in Fig. 8. The theoretical curve in this case goes far above the measured points.

It should be noted that the experimental observation of the screen size effect is reported here for the first time. In fact, it was predicted [8] for far-infrared TR experiments but no attempts to compare experiment with the theory had been made.

Another important feature of DR is the dependence of radiation intensity on the position of the electron beam with respect to the centre of the slit. Figure 9 shows the detector I signal while scanning a slit of 10 mm width across the beam, together with

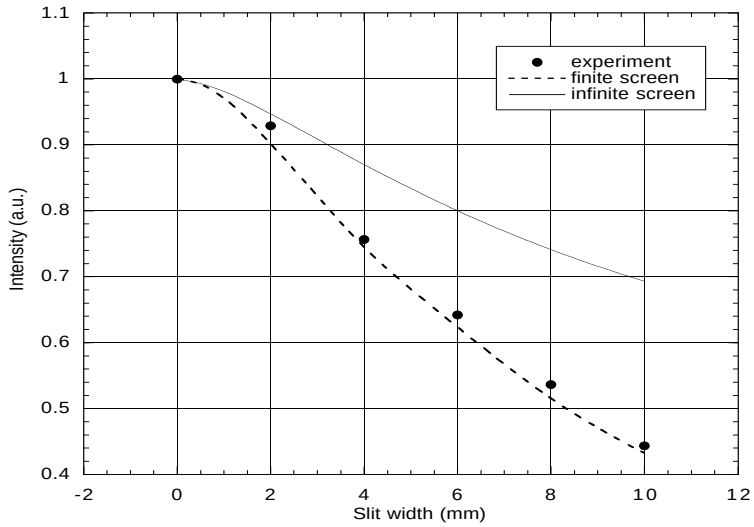

Figure 8: The normalized radiation power as a function of the slit aperture: experimental points and curves according to the infinite screen and far-filed theory (Ref. [11]), and the model taking into account screen size and corrections to the far-field approximation.

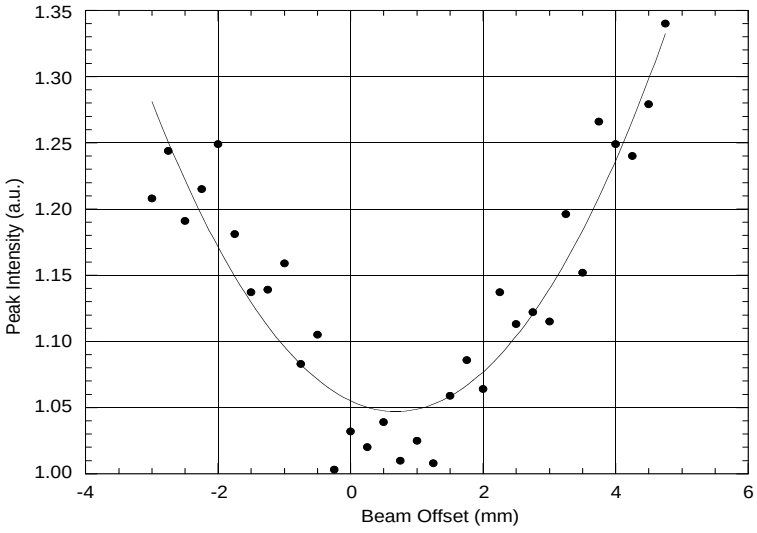

Figure 9: Coherent radiation intensity versus the beam position with the respect to the center of the 10 mm width slit.

the theoretical curve. This property of DR can be used to centre a slit on the beam even without any imaging device. This will be particularly useful when the beam energy and intensity make it impossible to use intercepting radiators.

4.2 Bunch length evaluation

The main goal of this paper is not to report of a very precise measurement of the bunch length, but rather to compare bunch length measurements done using TR case to those done using DR from different slit widths, under as much identical as possible experimental conditions. For this reason we will not take into account factors such as detector efficiency and transmission efficiency through the interferometer that, being common to TR and DR, do not introduce any difference between the two. In addition, to extract information on the bunch length from the inteferograms we follow the simple technique of Ref. [14]. The essence of the method consists in assuming the general bunch shape is known and working backwards to derive the power spectrum to be compared to the measured one. Further simplifications are to assume that the incoherent radiation frequency distribution is flat and to simulate the low frequency cut-off by introducing ad-hoc filter function.

We note that in the case of DR from a finite-size screen the last two assumptions are well justified by the shape of the computed spectrum (see Fig.6).

Previous measurements at TTF [15] using the Kramers-Kronig method to reconstruct the longitudinal bunch profile [16], gave evidence for a nearly rectangular bunch shape. We therefore assume that the bunch density distribution, $\rho(z)$, is a rectangle with sides smoothed by the convolution with a single Gaussian, namely

$$\begin{aligned} \rho(z) &= \frac{1}{\sqrt{2\pi}\delta}\int_{-\infty}^{\infty} u(z-z_0)e^{-z_0^2/2\delta^2}dz_0 \ , \\ u(z) &= \begin{cases} 1/\sigma & ,|z| \le \sigma/2 \\ 0 & ,|z| > \sigma/2 \end{cases} \ . \end{aligned} \tag{5}$$

Depending on the values of parameters σ and δ in Eq. (5), the assumed bunch shape can be continuously changed from pure rectangular to gaussian. We furthermore introduce the same filter function as used in reference [14],

$$g(\omega) = 1 - e^{-(\xi\omega/c)^2} \ , \tag{6}$$

with ξ a cut-off parameter, mostly because it allows to easily obtain an analytical expres-

sions for the radiation frequency spectrum and the autocorrelation function, respectively

$$I(\omega) \propto \frac{e^{-(\delta\omega/c)^2} \sin^2 \frac{\sigma\omega}{2c}}{\sigma^2\omega^2} \left(1 - e^{-(\xi\omega/c)^2}\right)^2 \ , \tag{7}$$

$$\begin{aligned} I(s) \ &\propto \ \zeta(\sigma - s, \delta) - 2\zeta(\sigma - s, \sqrt{\delta^2 + \xi^2}) + \zeta(\sigma - s, \sqrt{\delta^2 + 2\xi^2}) \\ &- \ 2\left[\zeta(s, \delta) - 2\zeta(s, \sqrt{\delta^2 + \xi^2}) + \zeta(s, \sqrt{\delta^2 + 2\xi^2})\right] \\ &+ \ \zeta(\sigma + s, \delta) - 2\zeta(\sigma + s, \sqrt{\delta^2 + \xi^2}) + \zeta(\sigma + s, \sqrt{\delta^2 + 2\xi^2}) \ , \end{aligned} \tag{8}$$

$$\zeta(t, \tau) = 2\tau e^{-t^2/4\tau^2} + \sqrt{\pi}\, t\, \mathrm{erf}(t/2\tau) \ , \tag{9}$$

where erf(x) is the error function.

By fitting the autocorrelation curve to the measured data we obtained best estimations for σ, δ and ξ.

An example of the fit is shown in Fig. 10 ; the best fit (fit 1) to the measured data is quite good on the central peak, that carries the most relevant informations on bunch length, but gets worse in the tails. The source of this discrepancy is in the shape of the filter function described by Eq. (6) that falls off smoothly with ω while the measured spectra (see Fig. 6) are truncated sharply at a frequency ω_t below which the intensity becomes essentially negligible. The model is therefore expected to improve if Eq. (6) is, for instance,multiplied by the step function

$$\theta(\omega_t) = \begin{cases} 1 & ,\omega \geq \omega_t \\ 0 & ,\omega < \omega_t \end{cases} \ . \tag{10}$$

Because an analytical expression for the autocorrelation curve can not be obtained in this case, a numerical calculation was performed using as filter function the product of Eq. (7) and Eq. (10) with ω_t = 0.38 THz·rad ; the result is shown in Fig.10 (fit 2). Note that the bunch length estimated from the fit is almost completely insensitive to the choice of the filter function.

Values of the reconstructed bunch length σ and of the cut-off parameter ξ , obtained from fits to all measured data sets, are plotted in Fig. 11 versus slit width. The bunch length changes by less than 3% over the whole range of widths, a variance much smaller then the expected systematic error. The cut-off parameter varies by ≈15% and its dependence on the slit width is in qualitative agreement with theoretical calculations predicting a continuous shift of the spectrum cut-off towards lower frequencies (Fig. 6) as the slit width increases. The smoothing parameter, δ was in the range 30 μm to 80 μm (however its error was estimated to be larger then 100%)

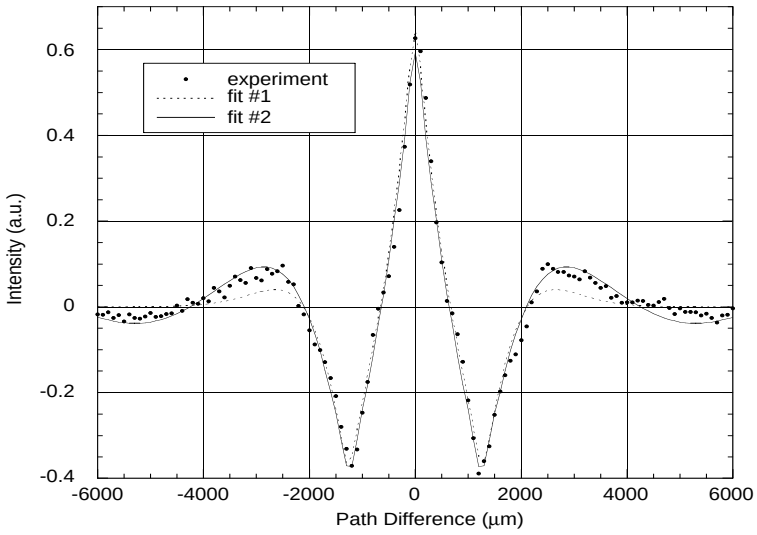

Figure 10: Fits of model autocorrelation curves to the experiment. Fit #1 uses a continuous filter function while in fit #2 the filter function is set to zero if $\omega < \omega_t$=0.38 THz·rad.

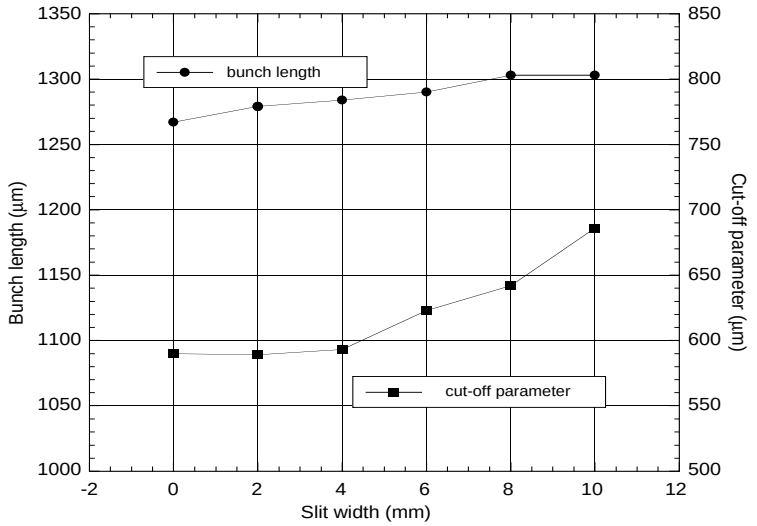

Figure 11: The bunch length and the cut-off parameter versus the slit width.

5 CONCLUSIONS

Measurements of coherent diffraction radiation generated by short electron bunches passing through a slit in a metal radiator were performed in the millimeter and submillimeter range using a Martin-Puplett interferometer. A specially designed diffraction radiator allowed us to collect data at different slit widths and compare DR and transition radiation under the same experimental conditions .

Experimental radiation spectra and intensities for different slit widths are also compared with theoretical predictions. We demonstrate that the conventional ideal model for infinite radiator and far-field conditions does not fit the measured data.

A more realistic model, taking into account the finite size of the radiator and the actual radiation collection geometry, is presented to give a good fit.

The bunch length is also evaluated using a conventional deconvolution technique, and simple models for the bunch shape and the measured radiation spectral distribution. The analysis shows that the reconstructed bunch length is almost completely insensitive to the slit width over a wide range of values including zero (TR mode).

Diffraction radiation is thus proved to be an effective, essentially non-intercepting tool for beam diagnostics purposes.

6 Acknowledgments

The strong support given by Prof. P.Schmüser is heartily acknowledged. The help of R.Sorchetti, who designed and installed the diffraction radiation slit, was fundamental for the success of the experiment.

References

[1] G.P.Williams, C.J.Hirschmugl, E.M.Kneedler, P.Z. Takacs, M.Shleifer, Y.J.Chabal and F.M.Hoffman, Phys. Rev. Lett. **62**, 261 (1989).

[2] K.Ishi, Y. Shibata, T.Takahashi, H.Mishiro, , M.Ikezawa, Y.Kondo, T. Nakazato, S. Urasawa, N. Niimura, R.Kato, Y.Shibasaki and M.Oyamada, Phys. Rev. A **43**, 5597 (1991).

[3] U.Happek, A.J.Sievers and E.B.Blum, Phys. Rev. Lett. **67**, 2962 (1991).

[4] Y.Shibata, K.Ishi, T.Takahashi, T.Kanai, M.Ikezawa, K.Takami, T.Matsuyama, K.Kobayashi and Y.Fujita, Phys. Rev. A **45**, 8340 (1992).

[5] M.Castellano, TESLA Reports 96-08, 1996.

[6] Barry, in *Beam Instrumentation*, edited by A.H.Lumpkin and C.E.Eyberger, AIP Conf. Proc., No. 390 (AIP, New York, 1997), p.173.

[7] Y.Shibata, S.Hasebe, K.Ishi, T.Takahashi, T.Ohsaka, M.Ikezawa, T. Nakazato, M.Oyamada, S. Urasawa, T.Yamakawa and Y.Kondo, Phys. Rev. E **52**, 6787 (1995).

[8] N.F.Shul'ga and S.N.Dobrovol'skii, Pis'ma Zh. Eksp. Teor. Fiz., **65**, 581 (1997) [JETP Lett. **65**, 611 (1997)]. N.F. Shul'ga, S.N. Dobrovol'skii and V.G. Syshchenko, Nucl. Instrum. & Methods in Phys. Res., Sect. B **145**, 180 (1998).

[9] B.M. Bolotovskii and G.V.Voskresenskii, Usp. Fiz. Nauk **88**, 209 (1966) [Sov. Phys. Dokl. **9**, 73 (1966)].

[10] F.G.Bass and V.M.Yakovenko, Usp.Fiz.Nauk **86**, 189 (1965) [Sov.Phys.Dokl. **8**, 420 (1965)].

[11] M.L. Ter-Mikaelian, *High-Energy Electromagnetic processes in Condensed Media* (Wiley-Interscience, New-York,1972).

[12] A.P.Potylitsin, Nucl. Instrum. Methods Phys. Res., Sect. B **145**, 169 (1998).

[13] M.Castellano, A.Cianchi, G.Orlandi and V.A.Verzilov, Nucl. Instrum. Methods Phys. Res., Sect. A **435**, 207 (1999).

[14] A.Murokh, J.B.Rosenzweig, M.Hogan, H.Suk, G.Travich and U.Happek, Nucl. Instrum. Methods Phys. Res., Sect. A **410**, 452 (1998).

[15] B Leissner, Ch. Berger, R. Siedling, M. Tonutti, M. Geitz, G. Schmidt, P. Schmuser, in *Proceedings of the 1999 Particle Accelerator Conference*, edited by A. Luccio and W. MacKay, (New York, 1999) p.2172.

[16] R. Lai and A.J. Sievers, Phys. Rev. E **50**, 3342 (1994).